Particle-localized ground state of atom-molecule Bose-Einstein condensates in a double-well potential

Atsushi Motohashi and Tetsuro Nikuni
Department of Physics, Tokyo University of Science, 1-3 Kagurazaka, Shinjuku-ku, Tokyo 162-8601, Japan
(Received 15 June 2010; published 30 September 2010)

We study the effect of atom-molecule internal tunneling on the ground state of atom-molecule Bose-Einstein condensates in a double-well potential. In the absence of internal tunneling between atomic and molecular states, the ground state is symmetric, which has equal-particle populations in two wells. From the linear stability analysis, we show that the symmetric stationary state becomes dynamically unstable at a certain value of the atom-molecule internal tunneling strength. Above the critical value of the internal tunneling strength, the ground state bifurcates to the particle-localized ground states. The origin of this transition can be attributed to the effective attractive interatomic interaction induced by the atom-molecule internal tunneling. This effective interaction is similar to that familiar in the context of BCS-BEC crossover in a Fermi gas with Feshbach resonance. Furthermore, we point out the possibility of reentrant transition in the case of the large detuning between the atomic and molecular states.

DOI: 10.1103/PhysRevA.82.033631 PACS number(s): 67.85.Hj, 67.60.Bc, 03.75.Lm

I. INTRODUCTION

Bose-Einstein condensation in dilute atomic gases has been offering opportunities to research macroscopic quantum phenomena since its experimental realization in 1995. In particular, one of the most fascinating macroscopic quantum phenomena is the Josephson effect between two Bose-Einstein condensates (BECs) trapped in a double-well potential. This system is called as a boson Josephson junction (BJJ) [1]. Recently, BJJs have been realized experimentally, and macroscopic wave functions are observed directly [2]. This experimental achievement has triggered much interesting research [3–5]. Though in BJJs the spatial coherence of BECs is focused, Josephson effects occur not only between spatially separated BECs but also between internal degrees of freedom in a single BEC. In particular, Josephson-like effects between atomic and molecular states have been discussed theoretically [6–8].

In the past decade many efforts have been devoted to creating molecular BECs from ultracold atoms [9–13]. Already molecular BECs have been created from fermionic atoms using magnetic Feshbach resonances [11]. On the other hand, the creation of coexisting atomic and molecular condensates by means of photoassociation has been discussed theoretically [14–16]. Photoassociation permits precise control of population transfer between individual discrete quantum states [17]. Currently, a mixture of a Rb BEC and a degenerate gas of Rb_2 ground-state molecules has been realized using photoassociation [13]. Furthermore, though not in a Bose-Einstein condensed phase, the collective oscillation of the populations between an atomic state and a molecular state has been observed [10,18,19]. The realization of atom-molecule BECs is forthcoming, and these experimental achievements have accelerated much theoretical research on atom-molecule coherence [20–25]. In particular it has been discussed that the atom-molecule internal tunneling changes the nature of system drastically. For instance, it is predicted that atom-molecule internal tunneling can induce a droplet-like ground state in atom-molecule BEC mixtures [6]. The relation between the Ising model and the phase transition of bosonic atom-molecule mixtures is also discussed [26–28]. As for atom-molecule mixtures in optical lattices, the possibility of a so-called super-Mott phase has been pointed out [29,30].

In this paper, we study atom-molecule BECs in a double-well potential by focusing on the effect of atom-molecule internal tunneling on the ground state. Although several authors have discussed BJJs of binary mixtures [31–34], the effects of internal degrees of freedom in BECs in a double-well potential have not been fully discussed. In the present paper, we consider atom-molecule internal tunneling. Even in a single-component BJJ, the competition between strengths of tunneling and interaction causes various phenomena such as macroscopic quantum self-trapping (MQST) [1]. Adding atom-molecule internal tunneling as a new degree of freedom, we will show that the competition between the atom-molecule internal tunneling and interwell tunneling or interaction leads to new phenomena.

As our main result, we will show that atom-molecule internal tunneling induces the asymmetric ground state, which has unequal particle populations in two wells. In the absence of internal tunneling, the ground state is symmetric, with equal particle populations in two wells. We note that ground states breaking the symmetry of trapping potentials have been found in various BEC systems. A well-known example of a symmetry-breaking ground state is a soliton in a quasi-one-dimensional attractive BEC [35,36]. The ground state in attractive BJJs also breaks the left-right symmetry of the double-well potential above a certain value of the interaction strength as predicted theoretically [37]. The asymmetric ground states in these systems are caused by attractive interactions. In contrast we will show that, even for repulsively interacting Bose gases, spontaneous symmetry breaking in the ground state emerges in atom-molecule BECs in a double-well potential owing to atom-molecule internal tunneling.

In addition, we show in the simplest case that the effect of atom-molecule internal tunneling can be described in terms of the effective interatomic attractive interaction. This effective interaction is similar to that familiar in the context of BCS-BEC crossover in a Fermi gas with Feshbach resonance [38].

We show that this effective interaction is always attractive and induces the asymmetric ground states in the absence of molecular tunneling, the intermolecule interaction, and the inter-atom-molecule interaction. Furthermore, we discuss the possibility of a reentrant transition, which cannot be explained by the simple form of the effective attractive interaction.

This paper is organized as follows. In Sec. II, we explain the model and approximations used in this paper. In Sec. II A, we introduce a four-mode model and classical analysis. In the four-mode model, we concentrate on condensate modes only and ignore other modes. Furthermore, we ignore quantum fluctuations by replacing creation-annihilation operators in the Hamiltonian by the c-number. Next, the parameters in this model are estimated from experiments.

In order to investigate the ground state, we first derive time-evolution equations in Sec. II B. Then, by using these equations, we derive the equations for the particle populations in the ground states in Sec. II C, and we develop the expression for eigenfrequencies in Sec. II D.

In Sec. III, we perform a linear stability analysis, using the equations derived in Sec. II. In particular, we investigate the stability of symmetric stationary states, where the particle numbers in the left and right wells are equal. By performing a linear stability analysis, we show that the atom-molecule tunneling induces the dynamical instability of the symmetric stationary state, which is the ground state in the absence of atom-molecule tunneling. This indicates the emergence of symmetry-breaking ground states, where the particles localize in one well. In Sec. III A, by using the equations for the particle populations in the ground state derived in Sec. II C, we show that this instability is accompanied by the bifurcation of symmetric stationary states to asymmetric ones. By comparing the energies of symmetric and asymmetric states, we confirm that the asymmetry state is the ground state. The general relation between dynamical instability and phase transition of ground states is discussed briefly in Appendix A. Some details of the calculations are given in Appendices B–E.

II. MODEL AND APPROXIMATIONS

A. Four-mode model and classical analysis

The second-quantized Hamiltonian for Bose atoms and molecules can be written as

$$\begin{aligned}\hat{H} = &\sum_{i=a,b}\int d\mathbf{r}\left(\frac{\hbar^2}{2m_i}\nabla\hat{\Psi}_i^\dagger\cdot\nabla\hat{\Psi}_i + V_{\rm ext}(\mathbf{r})\hat{\Psi}_i^\dagger\hat{\Psi}_i\right)\\ &+\frac{g_i}{2}\sum_{i=a,b}\int d\mathbf{r}\hat{\Psi}_i^\dagger\hat{\Psi}_i^\dagger\hat{\Psi}_i\hat{\Psi}_i + g_{ab}\int d\mathbf{r}\hat{\Psi}_a^\dagger\hat{\Psi}_b^\dagger\hat{\Psi}_b\hat{\Psi}_a\\ &-\lambda\int d\mathbf{r}(\hat{\Psi}_b^\dagger\hat{\Psi}_a\hat{\Psi}_a + \hat{\Psi}_a^\dagger\hat{\Psi}_a^\dagger\hat{\Psi}_b) + \delta\int d\mathbf{r}\hat{\Psi}_b^\dagger\hat{\Psi}_b, \qquad (1)\end{aligned}$$

where $\hat{\Psi}_a$ and $\hat{\Psi}_b$ represent field operators for Bose atoms and molecules, respectively, λ is the internal tunneling strength between atomic and molecular states, δ is the energy difference between atoms and molecules, and $V_{\rm ext}(\mathbf{r})$ is a double-well potential. The interatomic, the intermolecule, and the atom-molecule interactions can be approximated in terms of the s-wave scattering lengths as $g_i = 4\pi\hbar^2 a_{si}/m_i$ and $g_{ab} = 6\pi\hbar^2 a_{sab}/m_a$ $(i = a,b,m_b = 2m_a)$. Here, m_a is the mass of a Bose atom. Furthermore, we introduce the four-mode approximation. In this approximation, we concentrate on condensate modes only, and we ignore the effect of the particles occupying other modes. From this point of view, field operators can be approximated as $\hat{\Psi}_a \simeq \Phi_{aL}\hat{a}_L + \Phi_{aR}\hat{a}_R$ and $\hat{\Psi}_b \simeq \Phi_{bL}\hat{b}_L + \Phi_{bR}\hat{b}_R$, where Φ_{aL},Φ_{aR} (Φ_{bL},Φ_{bR}) are the wave functions of the atomic (molecular) condensate modes in the left well and the right well, respectively. $\hat{a}_L,\hat{a}_R$ $(\hat{b}_L,\hat{b}_R)$ are annihilation operators for the atomic (molecular) condensate modes in the left well and the right well, respectively. Applying these approximations to Eq. (1), we obtain the quantum four-mode Hamiltonian (four-mode model)

$$\begin{aligned}\hat{H} = &-J_a(a_L^\dagger a_R + a_R^\dagger a_L) - J_b(b_L^\dagger b_R + b_R^\dagger b_L)\\ &+\Delta(b_L^\dagger b_L + b_R^\dagger b_R) + \frac{U_a}{2}(a_L^\dagger a_L^\dagger a_L a_L + a_R^\dagger a_R^\dagger a_R a_R)\\ &+\frac{U_b}{2}(b_L^\dagger b_L^\dagger b_L b_L + b_R^\dagger b_R^\dagger b_R b_R)\\ &+U_{ab}(a_L^\dagger a_L b_L^\dagger b_L + a_R^\dagger a_R b_R^\dagger b_R)\\ &-g(b_L^\dagger a_L a_L + b_R^\dagger a_R a_R + a_L^\dagger a_L^\dagger b_L + a_R^\dagger a_R^\dagger b_R), \qquad (2)\end{aligned}$$

where the parameters are defined in Appendix B. In addition, we use classical analysis, in which annihilation operators are replaced by the c number $\sqrt{N}e^{i\theta}$, where N is the particle number of a condensate mode and θ is its phase. This approximation is justified when an occupation number is macroscopic. Using this procedure, we obtain the classical four-mode Hamiltonian as

$$\begin{aligned}H_{\rm cl} = &-2J_a\sqrt{N_{aL}N_{aR}}\cos(\theta_{aR}-\theta_{aL})\\ &-2J_b\sqrt{N_{bL}N_{bR}}\cos(\theta_{bR}-\theta_{bL}) + \Delta(N_{bL}+N_{bR})\\ &+\frac{U_a}{2}\left(N_{aL}^2+N_{aR}^2\right)+\frac{U_b}{2}\left(N_{bL}^2+N_{bR}^2\right)\\ &+U_{ab}(N_{aL}N_{bL}+N_{aR}N_{bR})\\ &-2g[N_{aL}\sqrt{N_{bL}}\cos(2\theta_{aL}-\theta_{bL})\\ &+N_{aR}\sqrt{N_{bR}}\cos(2\theta_{aR}-\theta_{bR})], \qquad (3)\end{aligned}$$

where N_{aL} (N_{aR}) represents the particle number of the atom in the left (right) well, and $N_{bL(bR)}$ represents that of the molecule in the left (right) well. θ_{aL} (θ_{aR}) is the phase of the atomic condensate in the left (right) well, and θ_{bL} (θ_{bR}) is the phase of the molecular condensate in the left (right) well.

In order to relate our model to realistic systems, we consider the double-well trap potential used in the experiment of a single-component BJJ of ^{87}Rb [2], and we set the parameters to be consistent with this experiment. In this experiment, the parameters are as follows: The ratio $\Lambda = NU_a/(2J_a)$ is estimated as 15 in Ref. [2], which corresponds to the strong-coupling case. Since the total-particle number N is 1150 in [2], the atomic interaction strength normalized by the atomic tunneling strength can be obtained as $U_a/J_a \simeq 3\times10^{-2}$. We use this value for the atomic interaction strength. As for the molecular interaction strength, we suppose that the molecular scattering length is the same as the atomic one and that the shapes of condensate wave functions of atoms and molecules are the same. Under this condition $U_b = U_a/2$ from Eq. (B4). In addition, in this study we set the total particle number as $N = N_{aL}+N_{aR}+2N_{bL}+2N_{bR} = 2000$.

We next consider the atom-molecule interaction. From the experiment [9], the atom-molecule scattering length of ^{87}Rb is estimated as $a_{am} = -180 \pm 150 a_0$, where a_0 is the Bohr radius, and the ratio of the atom-molecule scattering length and the atomic scattering length a_{am}/a_a can be estimated to range from about -3.2 to 0.3. Based on this value we suppose the atom-molecule interaction U_{ab} to be negative, but we treat it as a variable parameter. We will compare results with different values of U_{ab}. The negative U_{ab} is well suited to the internal tunneling between internal states because phase separation does not occur. This is different from a binary BEC mixture in the $|F = 2, m_f = 2\rangle$ and $|1, -1\rangle$ spin states of ^{87}Rb, where component separation is observed due to the repulsive interspecies interaction [39].

In order to set the molecular tunneling strength, we suppose that the atomic eigenstate Φ_{aL} (Φ_{aR}) and the molecular eigenstate Φ_{bL} (Φ_{bR}) have almost the same shapes. From Eq. (B1) and $m_b = 2m_a$, $J_b/J_a = 1/2$.

B. Equations of time evolution

In order to obtain the ground state and the eigenfrequencies corresponding to the excitation spectra, we derive the time-evolution equations. Using the classical four-mode Hamiltonian, we can derive the Hamilton equations of motion describing the dynamics of atomic and molecular BECs in a double-well potential as

$$\hbar \dot{N}_{aL} = \frac{\partial H_{\rm cl}}{\partial \theta_{aL}}, \quad \hbar \dot{N}_{aR} = \frac{\partial H_{\rm cl}}{\partial \theta_{aR}}, \tag{4}$$

$$\hbar \dot{N}_{bL} = \frac{\partial H_{\rm cl}}{\partial \theta_{bL}}, \quad \hbar \dot{N}_{bR} = \frac{\partial H_{\rm cl}}{\partial \theta_{bR}}, \tag{5}$$

$$\hbar \dot{\theta}_{aL} = -\frac{\partial H_{\rm cl}}{\partial N_{aL}}, \quad \hbar \dot{\theta}_{aR} = -\frac{\partial H_{\rm cl}}{\partial N_{aR}}, \tag{6}$$

$$\hbar \dot{\theta}_{bL} = -\frac{\partial H_{\rm cl}}{\partial N_{bL}}, \quad \hbar \dot{\theta}_{bR} = -\frac{\partial H_{\rm cl}}{\partial N_{bR}}. \tag{7}$$

These time-evolution equations can also be obtained by applying classical analysis to the Heisenberg equations derived from the quantum four-mode Hamiltonian. The Heisenberg equation and the Hamilton equation are related through the canonical commutation relation $[\hbar \hat{N}, \hat{\theta}] = i\hbar$ and the Poisson bracket $\{\hbar N, \theta\} = 1$. The explicit expressions of these equations are given in Appendix C.

C. Equations for the ground state

We now look for stationary solutions of the equations of motion for the particle numbers (C1)–(C4). We can easily find that the relative phases should be 0 in the ground states, that is, the atomic relative phase $\theta_{aL} - \theta_{aR} = 0$, the molecular relative phase $\theta_{bL} - \theta_{bR} = 0$, and the atom-molecule relative phases $2\theta_{aL(aR)} - \theta_{bL(bR)} = 0$, respectively.

In this study, we investigate the ground states in the presence of the atom-molecule internal tunneling in a symmetric double-well potential. From the Hamiltonian (3), the competition between the tunneling strengths and the interparticle interactions determines the ground states. The interwell tunnelings J_a and J_b lower the energy most when the particle populations are equal in the two wells. The interatomic and intermolecular repulsive interactions U_a and U_b act in the same way. In contrast to these contributions, the attractive atom-molecule interaction U_{ab} lowers the energy when the particles localize in one well. As discussed later in Sec. III B, the atom-molecule internal tunneling g can act effectively as an attractive interatomic interaction. This competition will create an asymmetric ground state, which breaks the symmetry of the double-well trap potential.

In order to look for the ground state with a fixed particle number, we introduce the chemical potential μ and the grand canonical energy

$$K \equiv H_{\rm cl} - \mu N, \tag{8}$$

where the total number is defined as $N = N_{aL} + N_{aR} + 2N_{bL} + 2N_{bR}$. Then the ground state can be determined from

$$\frac{\partial K}{\partial N_{aL(aR)}} = 0, \quad \frac{\partial K}{\partial N_{bL(bR)}} = 0, \tag{9}$$

or equivalently [from Eqs. (6) and (7)]

$$\hbar \dot{\theta}_{aL(aR)} = -\mu, \quad \hbar \dot{\theta}_{bL(bR)} = -2\mu. \tag{10}$$

From Eqs. (C5)–(C8), we obtain

$$-\mu = J_a \sqrt{\frac{N_{aR}}{N_{aL}}} - N_{aL} U_a - N_{bL} U_{ab} + 2g\sqrt{N_{bL}}, \tag{11}$$

$$-\mu = J_a \sqrt{\frac{N_{aL}}{N_{aR}}} - N_{aR} U_a - N_{bR} U_{ab} + 2g\sqrt{N_{bR}}, \tag{12}$$

$$-2\mu = J_b \sqrt{\frac{N_{bR}}{N_{bL}}} - \Delta - U_b N_{bL} - N_{aL} U_{ab} + g\frac{N_{aL}}{\sqrt{N_{bL}}}, \tag{13}$$

$$-2\mu = J_b \sqrt{\frac{N_{bL}}{N_{bR}}} - \Delta - U_b N_{bR} - N_{aR} U_{ab} + g\frac{N_{aR}}{\sqrt{N_{bR}}}. \tag{14}$$

These equations determine the stationary states. It is clear that these equations always have a symmetric solution $N_{aL} = N_{aR}, N_{bL} = N_{bR}$. However, the symmetric solution does not always have the lowest energy. We will show this in Sec. III from both the linear stability analysis and by calculating energy.

D. Excitation spectra

Solving the linearized Hamilton equations, we obtain the four eigenfrequencies of the excitation spectra from the stationary states. We will look at these eigenfrequencies to investigate the stability of the system. If the excitation frequency ω has an imaginary part, such a stationary state is dynamically unstable; that is, if the stationary state is perturbed slightly, the small-amplitude oscillation exponentially grows in time.

Our procedure is summarized as follows. We first expand $H_{\rm cl}$ in fluctuations around the symmetric stationary state to second order. Next, by performing the canonical transformation $(\theta_{aL},\theta_{aR},\theta_{bL},\theta_{bR}) \to (\tilde{\phi}_0,\tilde{\phi}_{AM},\tilde{\phi}_+,\tilde{\phi}_-)$ and $(N_{aL},N_{aR},N_{bL},N_{bR}) \to (\tilde{X}_0,\tilde{X}_{AM},\tilde{X}_+,\tilde{X}_-)$, we diagonalize the canonical momentum part of the Hamiltonian. Details of calculations are given in Appendix D. We arrive at the quadratic Hamiltonian

$$H_{\rm cl} \simeq \tfrac{1}{2}\tilde{\phi}_0^2 + \tfrac{1}{2}\tilde{\phi}_{AM}^2 + \tfrac{1}{2}\tilde{\phi}_+^2 + \tfrac{1}{2}\tilde{\phi}_-^2 + V_{\rm eff}(\tilde{X}_+,\tilde{X}_-,\tilde{X}_{AM}). \tag{15}$$

The explicit form of $V_{\rm eff}$ is given by

$$V_{\rm eff}(\tilde{X}_+,\tilde{X}_-,\tilde{X}_{AM}) \simeq gN_a\sqrt{N_b}\left[4U_a + U_b - 4U_{ab} + \frac{g}{\sqrt{N_b}}\left(4 + \frac{N_a}{2N_b}\right)\right] \times (\delta\tilde{X}_{AM})^2 + (\delta\tilde{X}_+,\delta\tilde{X}_-)\mathbf{V}\begin{pmatrix}\delta\tilde{X}_+\\ \delta\tilde{X}_-\end{pmatrix}, \tag{16}$$

where $N_a(N_b)$ is the atomic (molecular) particle number in each well at the symmetric stationary state, that is, $N_a \equiv N_{aL(aR)}, N_b \equiv N_{bL(bR)}$. The 2×2 matrix $\mathbf{V}$ is defined as

$$\mathbf{V} \equiv \begin{pmatrix} 2\Omega_+ Z_+\left(\alpha_+^2 J_a^e + J_b^e + 2\alpha_+ U_{ab}^e\right), & 2\sqrt{\Omega_+\Omega_- Z_+ Z_-}\left[-J_a^e + J_b^e + (\alpha_+ + \alpha_-)U_{ab}^e\right] \\ 2\sqrt{\Omega_+\Omega_- Z_+ Z_-}\left[-J_a^e + J_b^e + (\alpha_+ + \alpha_-)U_{ab}^e\right], & 2\Omega_- Z_-\left(\alpha_-^2 J_a^e + J_b^e + 2\alpha_- U_{ab}^e\right)\end{pmatrix}, \tag{17}$$

where $J_a^e \equiv J_a/N_a + U_a, J_b^e \equiv J_b/N_b + U_b^e$, and

$$U_b^e \equiv U_b + \frac{gN_a}{2N_b\sqrt{N_b}}, \quad U_{ab}^e \equiv \frac{g}{\sqrt{N_b}} - U_{ab}. \tag{18}$$

Using this quadratic Hamltonian, we obtain the linearized Hamilton equations. Eliminating the phase variables, we arrive at

$$\hbar^2\delta\ddot{\tilde{X}}_{AM} = -2gN_a\sqrt{N_b}\left(4U_a + U_b^e + 4U_{ab}^e\right)\delta\tilde{X}_{AM}, \tag{19}$$

$$\hbar^2\frac{d^2}{dt^2}\begin{pmatrix}\delta\tilde{X}_+\\ \delta\tilde{X}_-\end{pmatrix} = -2\mathbf{V}\begin{pmatrix}\delta\tilde{X}_+\\ \delta\tilde{X}_-\end{pmatrix}. \tag{20}$$

We then assume the normal mode solutions $\delta\tilde{X}_\pm \propto e^{\pm i\omega t}$, $\delta\tilde{X}_{AM} \propto e^{\pm i\omega t}$. Equation (19) immediately gives one eigenfrequency:

$$(\hbar\omega_{AM})^2 = 2gN_a\sqrt{N_b}\left(4U_a + U_b^e + 4U_{ab}^e\right) \tag{21}$$

The other two eigenfrequencies can be obtained by diagonalizing the coefficient matrix of Eq. (20):

$$(\hbar\omega_\pm)^2 = 2\left(AJ_a^e + CJ_b^e\right) + 4BU_{ab}^e \pm \sqrt{4\left[\left(AJ_a^e + CJ_b^e\right) + 2BU_{ab}^e\right]^2 - 16(AC - B^2)\left[J_a^e J_b^e - \left(U_{ab}^e\right)^2\right]}, \tag{22}$$

where we have defined the coefficients A, B, and C as $A \equiv N_a J_a + 2gN_a\sqrt{N_b}, B \equiv gN_a\sqrt{N_b}$, and $C \equiv N_b J_b + \frac{1}{2}gN_a\sqrt{N_b}$, respectively. We note that, from Eq. (D4), $\tilde{X}_{AM}$ and $\tilde{X}_\pm$ can be expressed in terms of number variables as

$$\tilde{X}_{AM} = \frac{N_b - 2N_a}{10\sqrt{gN_a\sqrt{N_b}}}. \tag{23}$$

$$\tilde{X}_\pm = \pm\frac{[(N_{aL} - N_{aR}) + \alpha_\mp(N_{bL} - N_{bR})]}{2(\alpha_+ - \alpha_-)\sqrt{2\Omega_\pm Z_\pm}}. \tag{24}$$

From Eq. (23), we see that the $\tilde{X}_{AM}$ mode represents the oscillation between atomic and molecular BECs. Therefore, ω_{AM} represents the internal Josephson frequency between atomic-molecular states. Since one can easily show $\alpha_+ > 0$ and $\alpha_- < 0$, Eq. (24) clearly shows that $\tilde{X}_+$ represents the out-of-phase interwell motion, in which the atoms and molecules oscillate inversely, whereas $\tilde{X}_-$ represents the in-phase interwell motion, in which the atoms and molecules oscillate in the same direction. For the parameters defined in Sec. II, $\omega_+(\omega_-)$ represents the out-of-phase (in-phase) mode. More generally, the eigenvectors of $\omega_\pm$ modes are the linear combination of in-phase and out-of-phase motions. In addition, the corresponding frequencies $\omega_\pm$ are reduced to the Josephson frequencies in the single-component case in the limit of $g \to 0$ and $U_{ab} \to 0$.

III. PARTICLE-LOCALIZED GROUND STATES INDUCED BY INTERNAL ATOM-MOLECULE TUNNELING

When the atom-molecule interaction U_{ab} and the atom-molecule internal tunneling g are small, the ground state is symmetric (i.e., the particle populations in two wells are equal to each other). In this section, we will show that the atom-molecule internal tunneling induces the particle-localized ground state. This transition from the nonlocalized ground state to the localized one is signaled by the dynamical instability of the in-phase mode. In what follows, we investigate the dynamical stability of the original symmetric ground state by using the excitation spectra derived in the previous section. After the stability analysis, we investigate the stationary states and show the bifurcation of the symmetric stationary state to the asymmetric ones. The cause of particle localization will be

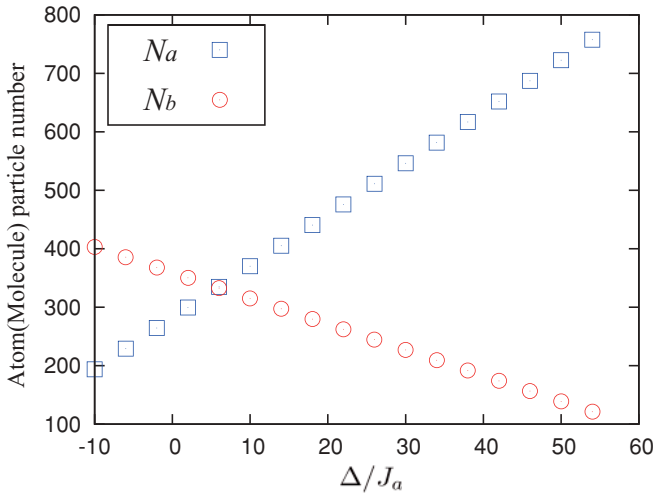

FIG. 1. (Color online) Δ dependence of particle populations in the symmetric stationary states. □ (◯) represents N_a (N_b).

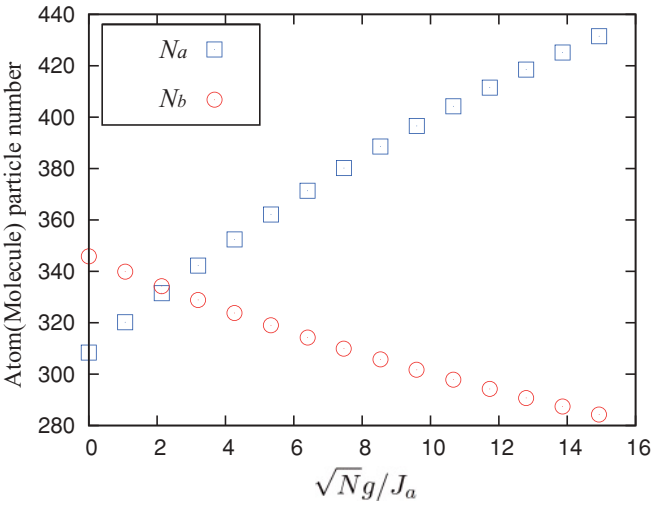

FIG. 2. (Color online) g dependence of particle populations in the symmetric stationary states. □ (◯) represents N_a (N_b).

discussed in Secs. III B and III C. In Secs. III C and III D, we also discuss the possibility of a reentrant transition.

Here, we explain the parameters of the particle interactions. We set the atomic interaction strength U_a and the molecular interaction strength U_b as described in Sec. II throughout this section. In what follows, we set the atom-molecule interaction strength as $U_{ab}/J_a = -2.3 \times 10^{-2}$ (except in the stability diagrams of Figs. 8 and 9 in which U_{ab} and g are varied), whose absolute value is slightly smaller than U_a.

A. Particle localization transition

First, we determine the atom-molecule energy difference Δ, which we use in this section. The stationary states are determined by solving Eq. (11)–(14). In the absence of atom-molecule internal tunneling there only exists the symmetric stationary state, which is the ground state. The Δ dependence of particle populations in the limit $g \to 0$ is shown in Fig. 1. From Fig. 1 each condensate has a few hundred particles so that the classical analysis introduced in Sec. II A is appropriate. Hereafter we choose the atom-molecule energy difference as $\Delta/J_a = 3$ in order that the atomic and molecular particle numbers be almost the same.

In Fig. 2, we investigate the g dependence of particle populations in the symmetric stationary state. From this figure we conclude that the particle populations are large enough for applying the mean-field approximation in a wide range of atom-molecule internal tunneling g. We also find that the atomic populations in the ground states grows, by increasing the atom-molecule internal tunneling strength. In the symmetric stationary state, where $2\theta_{aL(aR)} - \theta_{bL(bR)} = 0$, $N_a = N_{aL(aR)}$, and $N_b = N_{bL(bR)}$, the internal tunneling term in the Hamiltonian (3) is reduced to be $-4gN_a\sqrt{N_b}$. Because the order of N_a is larger than that of N_b, the symmetric stationary state tends to lower the total energy by increasing N_a rather than N_b in the large-g region.

Next, we investigate the dynamical stability of the symmetric stationary state by looking at the excitation frequencies. Figure 3 is the excitation spectra. ω_+ and ω_{AM} are always real and close to each other in the large-g region. On the other hand, as shown in Fig. 3, ω_- goes to zero at the finite atom-molecule internal tunneling g. As shown in Fig. 4, the imaginary part of ω_- emerges at the same value of g, while the other modes are still dynamically stable. This fact indicates the occurrence of a symmetry-breaking phase transition.

In order to confirm the appearance of the particle-localized ground state, we investigate the particle populations in the stationary state by solving Eqs. (11)–(14). Figures 5 and 6 show the atomic and molecular populations in the stationary solutions. These represent the bifurcation of the populations, which means the appearance of the new stationary states induced by the atom-molecule internal tunneling. In these new stationary states, the populations of atoms and molecules are localized in the same well, which means the breaking of the left-right symmetry of a double-well potential. The value of g at the bifurcation point is the same as that of the point where dynamical instability occurs. Furthermore, we compare the total energies of the symmetric and asymmetric ground states. Figure 7 shows that the total energy of the asymmetric state

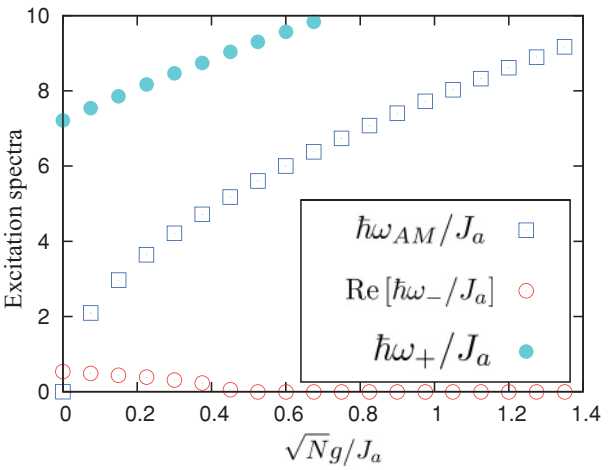

FIG. 3. (Color online) g dependence of excitation spectra of the symmetric stationary states.

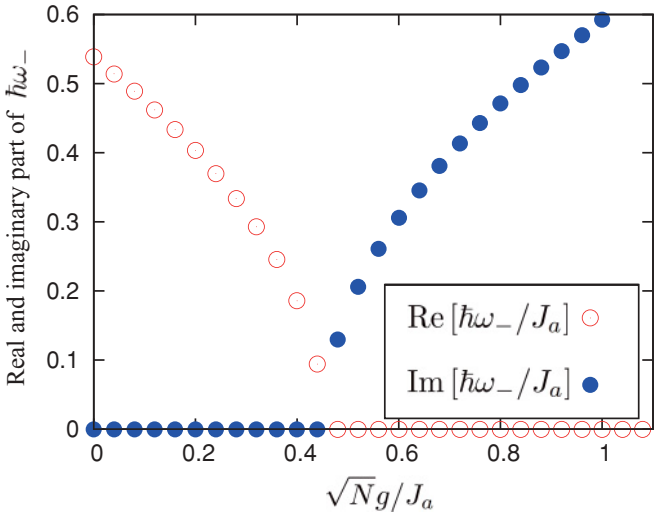

FIG. 4. (Color online) g dependence of imaginary part and real part of $\hbar\omega_-$ of symmetric stationary states.

is lower than that of the symmetric state, which means the alteration of the ground state.

Finally, we investigate the stability of symmetric stationary states by varying U_{ab} and g. The stability diagram of the symmetric stationary state is presented in Fig. 8. From this figure, the large g and negative U_{ab} induce the asymmetric ground state.

B. The effective attractive interaction

The effective interatomic attractive interaction mediated by molecular bosons is often discussed in the context of BCS-BEC crossover in a Fermi gas with Feshbach resonance using the two-channel model [38]. We discuss the same type of attractive interaction in the four-mode model, assuming the simplest case $J_b = U_b = U_{ab} = 0$.

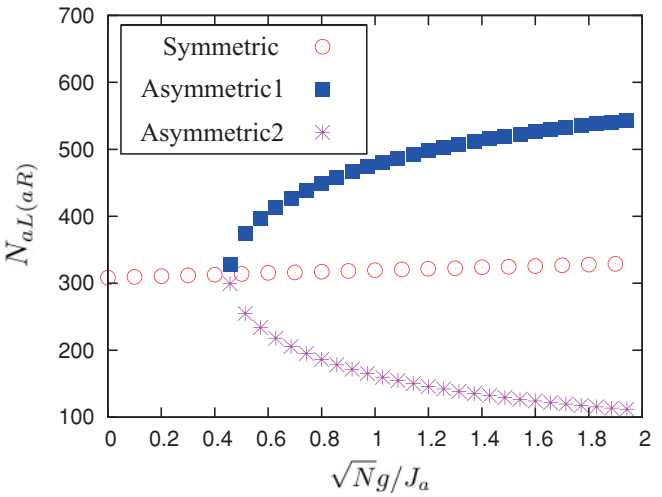

FIG. 5. (Color online) g dependence of atomic particle populations in the symmetric and asymmetric stationary states.

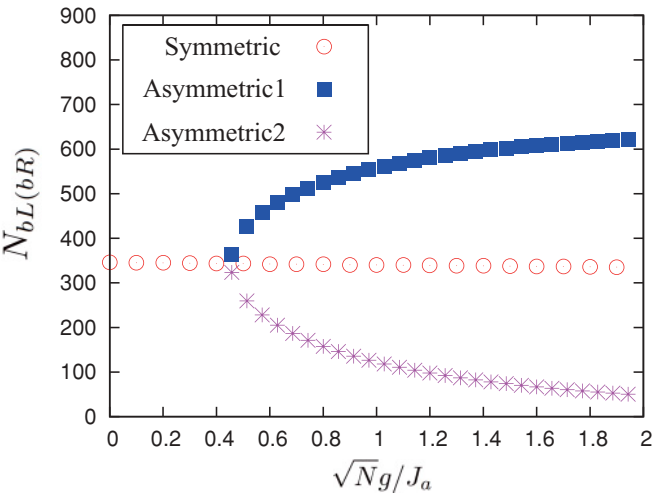

FIG. 6. (Color online) g dependence of molecular particle populations in the symmetric and asymmetric stationary states.

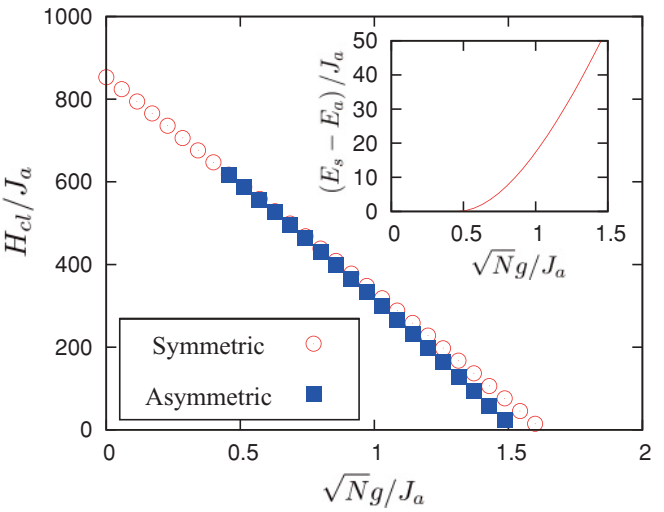

FIG. 7. (Color online) g dependence of total energy of the symmetric and asymmetric stationary states. The inset is the energy difference between symmetric and asymmetric stationary states. E_s (E_a) represents the total energy of the symmetric (asymmetric) stationary state.

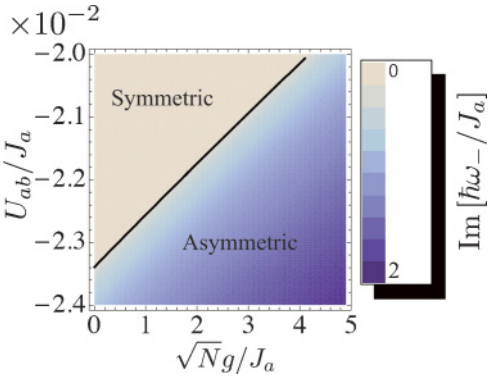

FIG. 8. (Color online) The stability phase diagram for the symmetric stationary state at $\Delta = 3J_a$. The black line represents $\hbar\omega_- = 0$.

In this simple case, we can solve Eqs. (13) and (14) for $\sqrt{N_{bL(bR)}}$ as

$$\sqrt{N_{bL(bR)}} = g\frac{N_{aL(aR)}}{\Delta - 2\mu}. \tag{25}$$

By using this in the grand canonical energy, we obtain

$$K = -2J_a\sqrt{N_{aL}N_{aR}} + \tfrac{1}{2}\tilde{U}_a\left(N_{aL}^2 + N_{aR}^2\right) - \mu(N_{aL} + N_{aR}), \tag{26}$$

where

$$\tilde{U}_a \equiv U_a - \frac{2g^2}{\Delta - 2\mu}. \tag{27}$$

This clearly shows that the effect of the atom-molecule tunneling modifies the interatomic interaction U_a to the effective interaction $\tilde{U}_a$. From Eq. (25), it is clear that $\Delta > 2\mu$ always. Therefore, *the contribution from the atom-molecule tunneling is always attractive in the case* $J_b = U_b = U_{ab} = 0$.

In order to investigate the transition from the symmetric to asymmetric state, we write

$$N_{aL} = N_a(1 + x), \quad N_{aR} = N_a(1 - x), \tag{28}$$

and we expand K in x. We obtain

$$K \simeq -2N_aJ_a + N_a^2\tilde{U}_a - 2\mu N_a + N_a(J_a + N_a\tilde{U}_a)x^2 + \frac{N_aJ_a}{4}x^4. \tag{29}$$

This clearly shows that the ground state is determined by the competition between the interwell tunneling J_a and the effective interaction $\tilde{U}_a$. The transition from the symmetric solution ($x = 0$) to the asymmetric solution ($x \neq 0$) occurs when the sign of the coefficient of the quadratic term changes from positive to negative. More explicitly, the asymmetric state become the ground state when $J_a + N_a\tilde{U}_a < 0$. By using (25), this condition is written as

$$J_a + N_aU_a < 2g\sqrt{N_b}. \tag{30}$$

From this condition, the atom-molecule tunneling always tend to make the asymmetric ground state. This analysis assumed the simple case $J_b = 0$, $U_b = 0$, and $U_a = 0$. One might expect that the quantitative results do not change for the general case, as long as J_b, U_b, and U_{ab} are small. However, in the following sections, we show that the atom-molecule tunneling also has the effect creating the symmetric ground state in the general case $J_b \neq 0$, $U_b \neq 0$, and $U_{ab} \neq 0$.

C. The stability condition of the symmetric stationary state

In this section, we consider the general case $J_b \neq 0$, $U_b \neq 0$, and $U_{ab} \neq 0$. In this case, we have not been able to reduce the ground canonical energy in a simple closed form in terms of atomic populations N_{aL} and N_{aR}. Thus, we use the excitation spectra in order to discuss the stability of the symmetric state.

From Eq. (22), the dynamical instability condition $(\hbar\omega_-)^2 < 0$ is reduced to be

$$\left(\frac{J_a}{N_a} + U_a\right)\left(\frac{J_b}{N_b} + U_b + \frac{gN_a}{2N_b\sqrt{N_b}}\right) < \left(-\frac{g}{\sqrt{N_b}} + U_{ab}\right)^2. \tag{31}$$

When this inequality is satisfied, the $\hbar\omega_-$ mode becomes dynamically unstable, signifying that the ground state becomes asymmetric. This condition generalizes Eq. (30) to including J_b,U_b, and U_{ab}. The remarkable difference from (30) is that the atom-molecule tunneling strength g appears on both sides of the equation. This means that the atom-molecule internal tunneling tends to create not only the asymmetric ground state but also the symmetric one. This nonmonotonic behavior has not been found in the simplest model neglecting J_b,U_b, and U_{ab}.

The term including g is $gN_a/(2N_b\sqrt{N_b})$ on the left-hand side, and $g/\sqrt{N_b}$ on the right-hand side. The ratio of these terms is $N_a/(2N_b)$, which is the ratio of the numbers of atomic-state and molecular-state particles. This is controlled by the atom-molecule energy difference Δ as in Fig. 1 and explained in Sec. III A.

The large Δ tends to increase N_a as seen from Fig. 1. Therefore, when $\Delta(>0)$ is large, by increasing g in Eq. (31), the term including g on the left-hand side is more enlarged than the one on the right-hand side. In contrast, when Δ is small, the term including g on the left-hand side does not have a significant role in the symmetric-asymmetric transition. Therefore, the atom-molecule tunneling tends to create an asymmetric ground state as Eq. (30).

However, this Δ dependence is not the case in the large-g region. Since the right-hand side is quadratic in g, the right-hand side of Eq. (31) is enlarged by g independently to the atom-molecule energy difference Δ in the large-g region. In this large-g region, Eq. (31) reduces to Eq. (30).

Therefore, when $\Delta(>0)$ is large, atom-molecule tunneling has a tendency to create a symmetric ground state in the small-g region, whereas it tends to create an asymmetric ground state in the large-g region. The influence of the atom-molecule tunneling on the ground state depends on the strength of the atom-molecule tunneling when $\Delta(>0)$ is large. In Sec III A, we investigated the small-Δ region. In the next section, we investigate the large-Δ region.

D. Reentrant transition

In this section, we discuss the possibility of reentrant transition, where the ground state changes in the order of asymmetric-symmetric-asymmetric by increasing g. Reentrant transition occurs when the positive Δ and the negative U_{ab} are large. As explained in the previous section, when $\Delta(>0)$ is large, atom-molecule tunneling tends to create a symmetric ground state in the small-g region. Therefore, when the negative U_{ab} is large enough to create an asymmetric ground state at $g = 0$, the finite g can cause the transition to the symmetric ground state from the asymmetric one. In contrast, in the large-g region, atom-molecule tunneling tends to create an asymmetric ground state, and the transition from symmetric to asymmetric ground state is possible. In this way, by increasing the internal tunneling g at a sufficiently large Δ, the ground state turns from the asymmetric state to the symmetric state, and again, goes to the asymmetric phase.

In fact, the large Δ changes the stability phase diagram to that shown in Fig. 9, which is quite different from Fig. 8. In this figure, around $U_{ab}/J_a = -2.5 \times 10^{-2}$ at $g = 0$, the symmetric stationary state is unstable, and increasing the

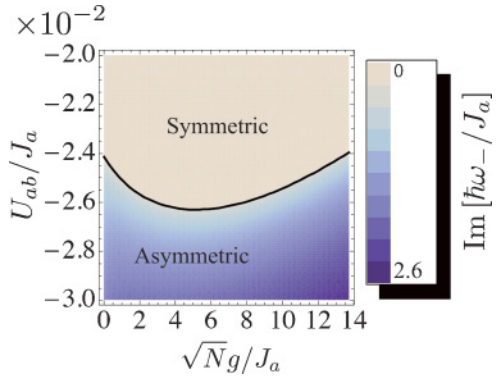

FIG. 9. (Color online) The stability phase diagram for the symmetric stationary state at $\Delta = 50J_a$. The black line represents $\hbar\omega_- = 0$.

internal tunneling g changes the symmetric state to a stable one. By increasing g further, the symmetric state turns to being unstable again. We note that asymmetric stationary states exist, when the symmetric state is unstable. In this region, the asymmetric states are the ground states.

In what follows, we estimate the value of Δ required to cause the reentrant transition at the ground state. From Eq. (31), the phase boundary between the stable and unstable phases is given by

$$U_{ab} = \frac{g}{\sqrt{N_b}} - \sqrt{\left(\frac{J_a}{N_a} + U_a\right)\left(\frac{J_b}{N_b} + U_b + \frac{gN_a}{2N_b\sqrt{N_b}}\right)}. \tag{32}$$

If the reentrant transition does not occur, the stability phase diagram is as shown in Fig. 8, where the phase boundary is almost a straight line. In contrast, in the case that the reentrant transition occurs as in Fig. 9, the phase boundary line has a minimal U_{ab} value. Therefore, from the condition $\partial U_{ab}/\partial g = 0$, we can derive the condition for reentrant transition. We find that

$$g_{\min} = \frac{1}{8\sqrt{N_b}}(J_a + N_aU_a) - \frac{2\sqrt{N_b}}{N_a}(J_b + N_bU_b), \tag{33}$$

where we define $g_{\min}$ as g at the minimal U_{ab} point. The condition for reentrant transition is given by $g_{\min} > 0$. In the weak-coupling limit $N_aU_a \ll J_a$ and $N_bU_b \ll J_b$, the condition $g_{\min} > 0$ is reduced to be $N_a/N_b > 16J_b/J_a$, and in the strong-coupling limit $N_aU_a \gg J_a$ and $N_bU_b \gg J_b$, the condition for reentrant transition is $N_a/N_b > 4\sqrt{U_b/U_a}$. In this paper, we take $NU_a/J_a = NU_b/J_b = 60$ following the discussion in Sec. II. Therefore, we are in the strong-coupling limit. Using the parameters in Sec. II, we have $U_b/U_a = 1/2$ and $N_a/N_b > 2\sqrt{2}$. By using this criterion, $\Delta \geqslant 40J_a$ is needed to cause the reentrant transition from Fig. 10.

We now examine the experimental possibility of realizing this large detuning Δ. First, we estimate the value of $J_a/\hbar$. Within a two-mode model, the Josephson frequency in the single-component case [1] is $\hbar\omega_J = 2J_a\sqrt{1+\Lambda}$. In the single BJJ experiment [2], the Josephson frequency is estimated as $\omega_J = 40(\text{ms})^{-1}$, and $\Lambda = 15$ as explained in Sec. II. Using these values, we find $J_a/\hbar \simeq 20\ \text{s}^{-1}$. Using this value, we

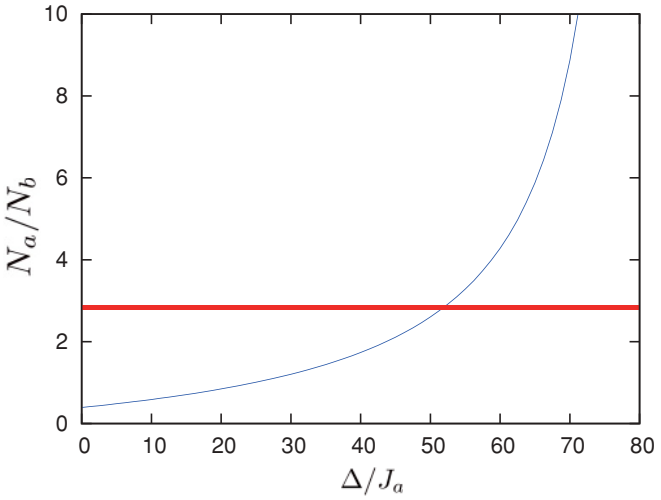

FIG. 10. (Color online) Δ dependence of N_a/N_b of the symmetric stationary state. The thick line represents $N_a/N_b = 2\sqrt{2}$.

estimate the value of $\Delta = 50J_a$, which we use in Fig. 9. This gives

$$\frac{\Delta}{\hbar} = 50 \times 20\ \text{s}^{-1} = 1\ \text{kHz}. \tag{34}$$

We compare this value with the experimental value of the Feshbach resonance using ^{87}Rb [19]. In this experiment, the energy difference between the open-channel (closed-channel), which corresponds to the atomic (molecular) state, is $\Delta\mu(B - B_{\text{res}})$, where $\Delta\mu$ is the difference of magnetic moments between these states, and B is the strength of the magnetic field. B_{res} is the strength of the magnetic field at the Feshbach resonance point. In this experiment, $\Delta\mu$ is estimated as $\Delta\mu = 2\pi\hbar \times 111\ \text{kHz/G}$. In this experiment, B ends up being typically 50 mG away from the Feshbach resonance. Using this value, we obtain $\Delta\mu \times (B - B_{\text{res}})/\hbar \simeq 2\pi \times 5$ kHz. This is larger than the estimated value given in (34).

IV. SUMMARY

We investigated how atom-molecule internal tunneling changes the ground state of atom-molecule BECs in a double-well potential. From the linear stability analysis, we showed that atom-molecule internal tunneling induces the particle-localized ground state through dynamical instability. This is quite different from the single-component BJJ because the tunneling terms between BECs tend to prevent localizations in a single-component BJJ [37].

As explained in Sec. III C the particle localization is caused by the fact that the interatom-molecule tunneling behaves like interatomic *attractive* interaction effectively. We showed that this effective interaction is always attractive in the absence of J_b, U_b, and U_{ab}. This is the same type of effective interaction as in the two-channel model often used in the study of BEC-BCS crossover in a Fermi gas with Feshbach resonance [38].

However, the situation can be quite different in the general case that $J_b \neq 0$, $U_b \neq 0$, and $U_{ab} \neq 0$. We pointed out the possibility of a reentrant transition, which cannot be understood in terms of the effective attractive interaction. In the large-$\Delta(>0)$ region, the ground state changes from localized

to nonlocalized, and again to localized, with increasing atom-molecule internal tunneling. From this result, we pointed out the possibility that atom-molecule internal tunneling exhibits the rich physics undiscovered in the treatment of the simple two-channel model neglecting atom-molecule and intermolecule interactions.

Next, we pointed out that quantum fluctuations do not prevent the particle localization. In order to consider the effect of quantum fluctuations, we performed the exact diagonalization of the Hamiltonian (2) [40]. From this full-quantum treatment, we conclude that the ground state becomes the superposition of the particle-localized states in the left and right well.

Finally, we note that the reentrant transition cannot occur in a binary BEC mixture. By replacing the internal tunneling term in the (2) with $(\hat{b}_L^\dagger \hat{a}_L + \hat{b}_L \hat{a}_L^\dagger + \hat{b}_R^\dagger \hat{a}_R + \hat{b}_R \hat{a}_R^\dagger)$, we have the Hamiltonian for a binary BEC mixture. From the same procedure as in Sec. II, we can obtain the equation for a binary BEC mixture similar to Eq. (31). From this equation, we can conclude that the reentrant transition is unique to atom-molecule mixture BECs.

ACKNOWLEDGMENTS

The authors would like to thank S. Konabe, S. Watabe, T. Miyakawa, S. Tsuchiya, I. Danshita, T. Kato, T. Yamamoto, T. Ozaki, J. Haruyama, and Y. Iwami for valuable comments and discussions.

APPENDIX A: DYNAMICAL INSTABILITY AND SECOND-ORDER PHASE TRANSITION

In this Appendix, we briefly review the general relation between symmetry breaking and dynamical instability. We suppose the classical Hamiltonian having f degrees of freedom as $H = \sum_{i=1}^{f} \frac{p_i^2}{2} + V_{\rm eff}(x_1, x_2, \ldots, x_f)$, where $x_i (i = 1, \ldots, f)$ are the dynamical variables and $p_i (i = 1, \ldots, f)$ are their canonical momenta. The coefficients of kinetic terms have been normalized by scaling the dynamical variables. Expanding this effective potential around stationary states to second order in the fluctuations, one obtains $H \simeq \sum_i^f \frac{p_i^2}{2} + \frac{1}{2}\sum_{i,j} \frac{\partial^2 H}{\partial x_i \partial x_j}\delta x_i \delta x_j \equiv \sum_i^f \frac{p_i^2}{2} + \frac{1}{2}\delta \mathbf{x}^\dagger \mathbf{V} \delta \mathbf{x}$. Here we defined $\delta \mathbf{x}^\dagger \equiv (\delta x_1, \delta x_2, \ldots, \delta x_f)$ and $\mathbf{V}_{i,j} \equiv \partial^2 H / \partial x_i \partial x_j$. The linearized Hamilton equations are given by $\dot{p}_i = -\frac{\partial H}{\partial x_i} = -\sum_{j=1}^f \frac{\partial^2 H}{\partial x_i \partial x_j}\delta x_j$, $\delta \dot{x}_i = \frac{\partial H}{\partial p_i} = p_i$, then $\delta \ddot{x}_i = -\sum_{j=1}^f \frac{\partial^2 H}{\partial x_i \partial x_j}\delta x_j \Leftrightarrow \delta \ddot{\mathbf{x}} = -\mathbf{V}\delta \mathbf{x}$. Defining the eigenfrequency as ω, with $x_i \propto e^{\pm i\omega t}$ $(i = 1, \ldots, f)$, we find that the eigenvalue of $\mathbf{V}$ is equal to ω^2.

It is thus clear that the matrix $\mathbf{V}$ is positive definite, if we expand around the ground state. Then, if any of eigenvalues change to be negative at a ground state by varying parameters, this state is no longer a ground state. In general, the original ground state becomes a saddle point or a local maximum, and the new ground states are bifurcated around the original one.

Consequently, the second-order phase transition of $V_{\rm eff}$ corresponds to the fact that an excitation spectrum $\hbar\omega$ becomes purely imaginary number. A purely imaginary ω represents a slipping off from the original ground state to the symmetry-breaking ones. Since $\mathbf{V}$ is the symmetric matrix, the eigenvalue is always real, and thus in this second-order phase transition of a ground state, an excitation spectra becomes a purely imaginary number.

APPENDIX B: PARAMETERS

The parameters are defined as follows:

$$J_i \equiv -\int d\mathbf{r}\Phi_{iL}^* \left[-\frac{\hbar^2}{2m_i}\nabla^2 + V_{\rm ext}(\mathbf{r})\right]\Phi_{iR}, \tag{B1}$$

$$E_i^0 \equiv \int d\mathbf{r}\Phi_{iL}^* \left[-\frac{\hbar^2}{2m_i}\nabla^2 + V_{\rm ext}(\mathbf{r})\right]\Phi_{iL} = \int d\mathbf{r}\Phi_{iR}^* \left[-\frac{\hbar^2}{2m_i}\nabla^2 + V_{\rm ext}(\mathbf{r})\right]\Phi_{iR}, \tag{B2}$$

$$U_i \equiv g_i \int d\mathbf{r}|\Phi_{iL}|^4 = g_i \int d\mathbf{r}|\Phi_{iR}|^4, \tag{B3}$$

$$U_{ab} \equiv g_{ab}\int d\mathbf{r}|\Phi_{aR}|^2|\Phi_{bR}|^2 = g_{ab}\int d\mathbf{r}|\Phi_{aL}|^2|\Phi_{bL}|^2, \tag{B4}$$

$$g \equiv \lambda \int d\mathbf{r}\Phi_{bL}^*\Phi_{aL}\Phi_{aL} = \lambda \int d\mathbf{r}\Phi_{bR}^*\Phi_{aR}\Phi_{aR}, \tag{B5}$$

$$\Delta \equiv \delta \int d\mathbf{r}|\Phi_{bL}|^2 + E_b^0 - 2E_a^0 = \delta \int d\mathbf{r}|\Phi_{bR}|^2 + E_b^0 - 2E_a^0, \tag{B6}$$

where $i = a$ (b) represents atomic (molecular) BEC modes, and L (R) expresses the left (right) well, respectively.

APPENDIX C: TIME-EVOLUTION EQUATIONS

The explicit forms of the Hamilton equations (4)–(7) are as follows:

$$\hbar\dot{N}_{aL} = -2J_a\sqrt{N_{aL}N_{aR}}\sin(\theta_{aR} - \theta_{aL}) + 4gN_{aL}\sqrt{N_{bL}}\sin(2\theta_{aL} - \theta_{bL}), \tag{C1}$$

$$\hbar\dot{N}_{aR} = -2J_a\sqrt{N_{aL}N_{aR}}\sin(\theta_{aL} - \theta_{aR}) + 4gN_{aR}\sqrt{N_{bR}}\sin(2\theta_{aR} - \theta_{bR}), \tag{C2}$$

$$\hbar\dot{N}_{bL} = -2J_b\sqrt{N_{bL}N_{bR}}\sin(\theta_{bR} - \theta_{bL}) - 2gN_{aL}\sqrt{N_{bL}}\sin(2\theta_{aL} - \theta_{bL}), \tag{C3}$$

$$\hbar\dot{N}_{bR} = -2J_b\sqrt{N_{bL}N_{bR}}\sin(\theta_{bL} - \theta_{bR}) - 2gN_{aR}\sqrt{N_{bR}}\sin(2\theta_{aR} - \theta_{bR}), \tag{C4}$$

$$\hbar\dot{\theta}_{aL} = J_a\sqrt{\frac{N_{aR}}{N_{aL}}}\cos(\theta_{aR} - \theta_{aL}) - N_{aL}U_a - N_{bL}U_{ab} + 2g\sqrt{N_{bL}}\cos(2\theta_{aL} - \theta_{bL}), \tag{C5}$$

$$\hbar\dot{\theta}_{aR} = J_a\sqrt{\frac{N_{aL}}{N_{aR}}}\cos(\theta_{aL} - \theta_{aR}) - N_{aR}U_a - N_{bR}U_{ab} + 2g\sqrt{N_{bR}}\cos(\theta_{bR} - 2\theta_{aR}), \tag{C6}$$

$$\hbar\dot{\theta}_{bL} = J_b\sqrt{\frac{N_{bR}}{N_{bL}}}\cos(\theta_{bR}-\theta_{bL}) - \Delta - N_{bL}U_b - N_{aL}U_{ab} + g\frac{N_{aL}}{\sqrt{N_{bL}}}\cos(2\theta_{aL}-\theta_{bL}), \tag{C7}$$

$$\hbar\dot{\theta}_{bR} = J_b\sqrt{\frac{N_{bL}}{N_{bR}}}\cos(\theta_{bL}-\theta_{bR}) - \Delta - N_{bR}U_b - N_{aR}U_{ab} + g\frac{N_{aR}}{\sqrt{N_{bR}}}\cos(2\theta_{a2}-\theta_{bR}). \tag{C8}$$

APPENDIX D: CANONICAL TRANSFORMATION

The relative phases in the ground state are $\theta_{aL(bL)} - \theta_{aR(bR)} = 0, 2\theta_{aL(aR)} - \theta_{bL(bR)} = 0$. Expanding cosines around these zero phases as $\cos\theta \simeq 1 - \frac{1}{2}\theta^2$, we obtain the quadratic form in the phase variables. Therefore, the classical Hamiltonian can be expanded to second order in phase fluctuations around the symmetric stationary state. Furthermore, we diagonalize the Hamiltonian about the phase fluctuations. As a result, one of the eigenvalues is zero, and therefore the number of degrees of freedom decreases by one. We avoid this problem by introducing a fictitious parameter α, and in the last of the calculations, we set $\alpha \to 0$. After these procedures, we obtain the Hamiltonian as

$$H_{\rm cl} \simeq \alpha\phi_0^2 + \tfrac{1}{2}U\phi_{AM}^2 + \Omega_+ Z_+\phi_+^2 + \Omega_- Z_-\phi_-^2 + V_{\rm eff}(N_{aL},N_{aR},N_{bL},N_{bR}), \tag{D1}$$

where

$$\Omega_\pm \equiv N_aJ_a + N_bJ_b + \tfrac{5}{2}gN_a\sqrt{N_b} \pm \tfrac{1}{2}\sqrt{4(N_aJ_a - N_bJ_b)^2 + 12(N_aJ_a - N_bJ_b)gN_a\sqrt{N_b} + 25g^2N_a^2N_b}, \tag{D2}$$

and $Z_\pm \equiv (2\alpha_\pm^2+2)^{-1}$, where $\alpha_\pm \equiv (\Omega_\pm - 2N_bJ_b - gN_a\sqrt{N_b})/(2gN_a\sqrt{N_b})$. We defined the following notation: $\phi_0 \equiv \frac{1}{2}\theta_{aL} + \frac{1}{2}\theta_{aR} + \theta_{bL} + \theta_{bR}$, $\phi_{AM} \equiv -2\theta_{aL} - 2\theta_{aR} + \theta_{bL} + \theta_{bR}$, and $\phi_\pm \equiv \alpha_\pm\theta_{aL} - \alpha_\pm\theta_{aR} - \theta_{bL} + \theta_{bR}$. ϕ_0 represents the whole increase of phases keeping the relative phases constant, $\phi_\pm$ are the interwell oscillation modes, and ϕ_{AM} is the oscillation between the atomic and molecular states. $V_{\rm eff}$ is

$$V_{\rm eff} = -2J_a\sqrt{N_{aL}N_{aR}} - 2J_b\sqrt{N_{bL}N_{bR}} + \Delta(N_{bL}+N_{bR}) + \frac{U_a}{2}\left(N_{aL}^2+N_{aR}^2\right) + \frac{U_b}{2}\left(N_{bL}^2+N_{bR}^2\right) + U_{ab}(N_{aL}N_{bL}+N_{aR}N_{bR}) - 2g[N_{aL}\sqrt{N_{bL}} + N_{aR}\sqrt{N_{bR}}]. \tag{D3}$$

We denote the canonical conjugate variables with ϕ_0, ϕ_+, ϕ_-, ϕ_{AM} as $X_i (i = 0, +, -, AM)$. These are related to the particle numbers as

$$\begin{pmatrix} X_0 \\ X_+ \\ X_- \\ X_{AM} \end{pmatrix} = \begin{pmatrix} \frac{1}{5} & \frac{1}{5} & \frac{2}{5} & \frac{2}{5} \\ \frac{1}{2}\xi & -\frac{1}{2}\xi & \frac{1}{2}\alpha_-\xi & -\frac{1}{2}\alpha_-\xi \\ -\frac{1}{2}\xi & \frac{1}{2}\xi & -\frac{1}{2}\alpha_+\xi & \frac{1}{2}\alpha_+\xi \\ -\frac{1}{5} & -\frac{1}{5} & \frac{1}{10} & \frac{1}{10} \end{pmatrix}\begin{pmatrix} N_{aL} \\ N_{aR} \\ N_{bL} \\ N_{bR} \end{pmatrix}, \tag{D4}$$

where $\xi \equiv (\alpha_+ - \alpha_-)^{-1}$. X_0 represents the increase of whole particle number, $X_\pm$ is the interwell oscillation mode, and X_{AM} is the oscillation between the atomic and molecular states. The Poisson brackets are $\{X_i,\phi_j\} = i\delta_{i,j} (i,j = 0, +, -, AM)$, and therefore these are canonical conjugate variables. We then rescale ϕ_0, $\phi_\pm$, ϕ_{AM} as $\tilde{\phi}_0 \equiv \sqrt{2\alpha}\phi_0, \tilde{\phi}_{AM} \equiv \sqrt{gN_a\sqrt{N_b}}\phi_{AM}$, $\tilde{\phi}_+ \equiv \sqrt{2\Omega_+Z_+}\phi_+$, $\tilde{\phi}_- \equiv \sqrt{2\Omega_-Z_-}\phi_-$. Corresponding canonical transformation for the coordinate variables are $\tilde{X}_0 \equiv X_0/\sqrt{2\alpha}$, $\tilde{X}_{AM} \equiv X_{AM}/\sqrt{gN_a\sqrt{N_b}}$, $\tilde{X}_+ \equiv X_+/\sqrt{2\Omega_+Z_+}$, $\tilde{X}_- \equiv X_-/\sqrt{2\Omega_-Z_-}$. It is easy to see that the Poisson brackets are maintained as $\{X_i,\phi_j\} = \{\tilde{X}_i,\tilde{\phi}_j\} = \delta_{i,j}$ $(i,j = 0,+,-,AM)$. Therefore this transformation is the canonical transformation. As a result of this procedure, *the αdependence of the coefficient of ϕ_0 moves to that of $\tilde{X}_0$*. By setting the fictitious parameter $\alpha \to 0$ and eliminating the degrees $\tilde{X}_0$ relating to global phase rotation, the degrees of the interwell and internal tunnelings are decoupled in $V_{\rm eff}$. Then, we finally arrive at the Hamiltonian (15) and (16).

APPENDIX E: LINEARIZED HAMILTON EQUATIONS

The linerarized Hamilton equations are $\hbar\delta\dot{\tilde{X}}_i = \partial H_{\rm cl}/\partial\tilde{\phi}_i = \tilde{\phi}_i$, where $i = 0, AM, \pm$, and

$$\hbar\dot{\tilde{\phi}}_0 = -\frac{\partial V_{\rm eff}}{\partial\tilde{X}_0} = -\alpha\left(U_a + 4U_b^e - 4U_{ab}^e\right)\delta\tilde{X}_0 - \sqrt{2\alpha C}\left(-2U_a + 2U_b^e + 3U_{ab}^e\right)\delta\tilde{X}_{AM}. \tag{E1}$$

$$\hbar\dot{\tilde{\phi}}_{AM} = -\frac{\partial V_{\rm eff}}{\partial\tilde{X}_{AM}} = -\sqrt{2\alpha C}\left(-2U_a + 2U_b^e + 3U_{ab}^e\right)\delta\tilde{X}_0 - 2C\left(4U_a + U_b^e + 4U_{ab}^e\right)\delta\tilde{X}_{AM} \tag{E2}$$

$$\hbar\dot{\tilde{\phi}}_\pm = -\frac{\partial V_{\rm eff}}{\partial\tilde{X}_\pm} = -4\Omega_\pm Z_\pm\left(\alpha_\pm^2 J_a^e + J_b^e + 2\alpha_\pm U_{ab}^e\right)\delta\tilde{X}_\pm - 4\sqrt{\Omega_+\Omega_-Z_+Z_-}\left(-J_a^e + J_b^e + (\alpha_+ + \alpha_-)U_{ab}^e\right)\delta\tilde{X}_\mp. \tag{E3}$$

By setting the fictitious parameter $\alpha \to 0$, the contribution from the degrees $\tilde{X}_0$ and $\tilde{\phi}_0$ relating to global phase rotation is eliminated.

[1] S. Raghavan, A. Smerzi, S. Fantoni, and S. R. Shenoy, Phys. Rev. A **59**, 620 (1999).
[2] M. Albiez, R. Gati, J. Fölling, S. Hunsmann, M. Cristiani, and M. K. Oberthaler, Phys. Rev. Lett. **95**, 010402 (2005).
[3] C. Weiss and N. Teichmann, Phys. Rev. Lett. **100**, 140408 (2008).
[4] V. S. Shchesnovich and M. Trippenbach, Phys. Rev. A **78**, 023611 (2008).
[5] D. Witthaut, F. Trimborn, and S. Wimberger, Phys. Rev. Lett. **101**, 200402 (2008).
[6] E. Timmermans, P. Tommasini, R. Côté, M. Hussein, and A. Kerman, Phys. Rev. Lett. **83**, 2691 (1999).
[7] G.-R. Jin, C. K. Kim, and K. Nahm, Phys. Rev. A **72**, 045602 (2005).
[8] G. Santos, A. Tonel, A. Foerster, and J. Links, Phys. Rev. A **73**, 023609 (2006).
[9] R. Wynar, R. S. Freeland, D. J. Han, C. Ryu, and D. J. Heinzen, Science **287**, 1016 (2000).
[10] E. A. Donley, N. R. Claussen, S. T. Thompson, and C. E. Wieman, Nature (London) **417**, 529 (2002).
[11] M. W. Zwierlein, C. A. Stan, C. H. Schunck, S. M. F. Raupach, S. Gupta, Z. Hadzibabic, and W. Ketterle, Phys. Rev. Lett. **91**, 250401 (2003).
[12] S. Dürr, T. Volz, A. Marte, and G. Rempe, Phys. Rev. Lett. **92**, 020406 (2004).
[13] K. Winkler, G. Thalhammer, M. Theis, H. Ritsch, R. Grimm, and J. H. Denschlag, Phys. Rev. Lett. **95**, 063202 (2005).
[14] M. Mackie, R. Kowalski, and J. Javanainen, Phys. Rev. Lett. **84**, 3803 (2000).
[15] H. Y. Ling, H. Pu, and B. Seaman, Phys. Rev. Lett. **93**, 250403 (2004).
[16] A. P. Itin and S. Watanabe, Phys. Rev. Lett. **99**, 223903 (2007).
[17] K. Bergmann, H. Theuer, and B. W. Shore, Rev. Mod. Phys. **70**, 1003 (1998).
[18] C. Ryu, X. Du, E. Yesilada, A. M. Dudarev, S. Wan, Q. Niu, and D. J. Heinzen, e-print arXiv:cond-mat/0508201.
[19] N. Syassen, D. M. Bauer, M. Lettner, D. Dietze, T. Volz, S. Dürr, and G. Rempe, Phys. Rev. Lett. **99**, 033201 (2007).
[20] P. D. Drummond, K. V. Kheruntsyan, and H. He, Phys. Rev. Lett. **81**, 3055 (1998).
[21] D. J. Heinzen, R. Wynar, P. D. Drummond, and K. V. Kheruntsyan, Phys. Rev. Lett. **84**, 5029 (2000).
[22] A. Vardi, V. A. Yurovsky, and J. R. Anglin, Phys. Rev. A **64**, 063611 (2001).
[23] T. Miyakawa and P. Meystre, Phys. Rev. A **71**, 033624 (2005).
[24] M. W. Jack and H. Pu, Phys. Rev. A **72**, 063625 (2005).
[25] T. Miyakawa and P. Meystre, Phys. Rev. A **74**, 043615 (2006).
[26] L. Radzihovsky, J. Park, and P. B. Weichman, Phys. Rev. Lett. **92**, 160402 (2004).
[27] M. W. J. Romans, R. A. Duine, S. Sachdev, and H. T. C. Stoof, Phys. Rev. Lett. **93**, 020405 (2004).
[28] M. J. Bhaseen, A. O. Silver, M. Hohenadler, and B. D. Simons, Phys. Rev. Lett. **103**, 265302 (2009).
[29] V. G. Rousseau and P. J. H. Denteneer, Phys. Rev. A **77**, 013609 (2008).
[30] V. G. Rousseau and P. J. H. Denteneer, Phys. Rev. Lett. **102**, 015301 (2009).
[31] S. Ashhab and C. Lobo, Phys. Rev. A **66**, 013609 (2002).
[32] C. Wang, P. G. Kevrekidis, N. Whitaker, and B. A. Malomed, Physica D **237**, 2922 (2008).
[33] I. I. Satija, R. Balakrishnan, P. Naudus, J. Heward, M. Edwards, and C. W. Clark, Phys. Rev. A **79**, 033616 (2009).
[34] B. Juliá-Díaz, M. Guilleumas, M. Lewenstein, A. Polls, and A. Sanpera, Phys. Rev. A **80**, 023616 (2009).
[35] R. Kanamoto, H. Saito, and M. Ueda, Phys. Rev. Lett. **94**, 090404 (2005).
[36] P. Ziń, B. Oleś, M. Trippenbach, and K. Sacha, Phys. Rev. A **78**, 023620 (2008).
[37] P. Ziń, J. Chwedeńczuk, B. Oleś, K. Sacha, and M. Trippenbach, Europhys. Lett. **83**, 64007 (2008).
[38] Y. Ohashi and A. Griffin, Phys. Rev. Lett. **89**, 130402 (2002).
[39] D. S. Hall, M. R. Matthews, J. R. Ensher, C. E. Wieman, and E. A. Cornell, Phys. Rev. Lett. **81**, 1539 (1998).
[40] A. Motohashi and T. Nikuni, J. Low Temp. Phys. **158**, 72 (2010).